

Analytical pyrolysis and thermal analysis to chemically characterise bitumen from Italian geological deposits and Neolithic stone tools

Federica Nardella*, Celia Duce, Erika Ribechini

Department of Chemistry and Industrial Chemistry, University of Pisa, Via Moruzzi 13, 56124 Pisa, Italy

Abstract

The chemical study of bitumen from stone tools from Italian Neolithic sites was carried out using analytical pyrolysis-based techniques, EGA-MS (evolved gas analysis mass spectrometry) and DSPy-GC/MS (double shot pyrolysis-gas chromatography/mass spectrometry). The study was mainly aimed at demonstrating the suitability of analytical pyrolysis for studying archaeological bitumen and for obtaining information regarding its origin. EGA-MS was employed to obtain information on the thermal complexity of the samples and on their thermal degradation areas and DSPy-GC/MS along with Principal Component Analysis (PCA) were tested for biomarker analysis to assess bitumen source in archaeological objects. Geological bituminous rocks from Central-Southern Italy were selected and used as reference materials to both optimize experimental parameters and to support data interpretation for archaeological samples.

Geological samples were also preliminary characterised by thermogravimetric analysis coupled with FTIR spectroscopy (TG-FTIR) under nitrogen and by TG analysis under oxygen to quantify their relative content of organic and inorganic species.

The combination of thermal analysis and analytical pyrolysis-based techniques allowed us to quantify the organic content of the bitumen samples and to obtain information on both soluble and insoluble organic fractions. In addition, the proposed approach highlighted the main degradative patterns and the main differences among samples coming from different geographical areas as well as differences between geological and archaeological bitumen. Finally, DSPy-GC/MS associated with PCA proved to be successful in assessing the bitumen source in archaeological objects by the detection of terpanes, distinctive biomarkers.

Keywords: Archaeological bitumen; biomarker analysis; analytical pyrolysis; thermal analysis

1. Introduction

1
2
3 Bitumen belongs to the class of fossil materials originated from crude oil by evaporation, polymerization
4
5 and maturation reactions over geological timescale [1]. Natural bitumen deposits are widespread in the
6
7 Middle-Eastern region although bitumen can be also found all over Europe [2–4]. The accessibility and
8
9 distinctive chemical-physical properties of this ubiquitous natural resource have made it one of the
10
11 materials of choice since the Middle Palaeolithic for many purposes (adhesive, hydro-repellent, coating and
12
13 sealing agents) [5–7].

14
15
16 Bitumen is a complex mixture of hydrocarbons and its chemical composition changes according to bitumen
17
18 origin because each natural deposit has a different genesis. This means that the chemical characterization
19
20 can allow us to establish the source of bitumen [8]. Two distinct classes of compounds can be mainly
21
22 identified, maltenes and asphaltenes. Maltenes are the most studied because they contain polycyclic
23
24 hydrocarbons such as terpanes and steranes, used as biomarkers for the chemical fingerprinting of
25
26 bitumen. Asphaltenes correspond to the more complex and heavy fraction of bitumen [9,10]. The
27
28 investigation of both maltenes and asphaltenes provides several information for bitumen source
29
30 identification and has been widely used for many application such as oil-oil and oil-source rock correlation,
31
32 evaluation of thermal maturity and degree of degradation and identification of the depositional
33
34 environmental conditions and type of biologic precursor [9,11]. The characterization of the samples at
35
36 molecular level is useful even in archaeological field because of the numerous information achievable. It
37
38 can provide criteria for correlation between archaeological bitumen and geological reference materials to
39
40 hypothesize the origin of the archaeological objects from which bitumen is collected [12].

41
42
43 In the last decade of the last century, several studies mainly based on GC/MS, GC-FID and IRMS have been
44
45 focused on bituminous materials characterization, in the field of archaeology and petroleum geochemistry
46
47 [13–16]. Procedures based on GC/MS, GC-FID and IRMS normally require sample quantities that are often
48
49 unavailable in the case of archaeological finds. In addition, such procedures entail several wet-chemical
50
51 sample pre-treatments leading to possible loss of analytes and contamination [17–19]. Thus, optimisation
52
53 of classical analytical protocols along with the employment of innovative and more efficient extraction
54
55
56
57
58
59
60
61
62
63
64
65

1 methods have been proposed [20]. In this framework, methods based on analytical pyrolysis (EGA-MS, Py-
2 GC/MS) have also demonstrated their suitability and versatility for studying samples from cultural heritage
3 [21,22]. They require significantly lower amounts of sample than those needed for gas chromatographic
4 analyses and they do not need any sample pre-treatment. In addition, analytical pyrolysis allows us to
5 obtain information simultaneously both on solvent soluble/hydrolysable and macromolecular fractions of
6 the same sample [23–25]. In particular, EGA-MS can be used to establish thermal degradation regions and
7 DSPy-GC/MS (double shot pyrolysis-gas chromatography/mass spectrometry) is able to accomplish thermal
8 desorption and high-temperature pyrolysis in two separate steps on the same sample. Thermogravimetric
9 analysis coupled to Fourier transform infrared spectroscopy (TG-FTIR) is also widely used to study
10 archaeological and artistic objects [26]. TG-FTIR is complementary to EGA-MS or DSPy-GC/MS allowing us
11 to quantify the mass loss associated to a pyrolytic decomposition, combustion and evaporation of a sample
12 and to estimate the relative content of inorganic and organic species [27–29]. The analysis of the evolved
13 gases by FTIR reveals the evolution of small molecules such as CO₂ and water that are not generally
14 acquired when using a mass spectrometer as a detector of pyrolysis products. However, despite all the
15 positive aspects of both thermal analysis and analytical pyrolysis, such techniques are rarely reported in the
16 study of bitumen and archaeological bitumen [30,31].

17
18 In this paper, we assess the appropriateness of TG-FTIR, EGA-MS and DSPy-GC/MS for the study of bitumen
19 and its biomarkers in both geological rocks from Central-Southern Italy and archaeological objects. The
20 geological bitumen samples were selected and used as reference materials to both optimize experimental
21 parameters and to support data interpretation for archaeological samples. In addition, principal component
22 analysis (PCA) was used to find out if a classification based on bitumen source can be obtained with the
23 information inferred from DSPy-GC/MS.

2. Materials and method

2.1. Samples

24 Table 1 lists the geological samples used as reference materials and the archaeological samples studied in
25 this work.

1
2 Natural bitumen was collected from caves located in Central – Southern Italy [32,33]; in particular in
3 Abruzzo (4 samples from Pescara and 2 samples from L’Aquila), Sicily (3 samples from Ragusa) and Lazio (1
4 sample from Frosinone). The samples occur as rocks in which bitumen is solid or semi-solid.
5

6
7 Archaeological bitumen was sampled from Neolithic flint flakes (about two centimetres long) dated back to
8
9 5800 – 5000 b.C. that showed spots of a thin layer of black organic material. The stone tools were collected
10
11 from archaeological excavations in Abruzzo in the Neolithic villages of Colle Cera and Catignano (Pescara)
12
13 [34,35]. All the samples studied were formerly analysed by an optimized method based on GC/MS [20].
14
15
16
17

18
19 **Table 1** – Geological and archaeological samples used in this study.
20

| | Sample | Location |
|-------------------------------|---------------|---------------------------|
| Geological bitumen | A1 | Abruzzo (PE) |
| | A2 | Abruzzo (PE) |
| | A3 | Abruzzo (PE) |
| | A4 | Abruzzo (AQ) |
| | A5 | Abruzzo (AQ) |
| | A6 | Abruzzo (PE) |
| | R1 | Sicily |
| | R2 | Sicily |
| | R3 | Sicily |
| | F | Lazio |
| Archaeological bitumen | CC6 | Colle Cera - Abruzzo (PE) |
| | CC7 | Colle Cera - Abruzzo (PE) |
| | CC9 | Colle Cera - Abruzzo (PE) |
| | CT1 | Catignano - Abruzzo (PE) |

2.2. Analytical procedures and instrumentation

2.2.1. TG-FTIR

23
24
25
26
27
28
29
30
31
32
33
34
35
36
37
38
39
40
41
42
43
44
45
46
47
48
49
50
51
52
53
54
55
56
57
58
59
60
61
62
63
64
65
Thermogravimetric analysis was performed using a TA Instruments Thermobalance Q500IR equipped with a spectrophotometer FTIR Agilent Technologies Cary 640 for evolved gas analysis. TG measurements were performed at a rate of 10 °C/min under nitrogen and air from 50 °C to 800 °C. TG-FTIR measurements were performed in the same temperature range at a rate of 20 °C/min, under nitrogen flow (70 mL/min), from 500 to 4000 cm⁻¹ with a resolution of 4 cm⁻¹. To reduce the strong background absorption from water and

1 carbon dioxide in the atmosphere, the optical bench was purged with nitrogen. In addition, a background
2 spectrum was taken before each analysis in order to zero the signal in the gas cell and to eliminate the
3
4 contribution due to the amount of ambient water and carbon dioxide. For each experiment, approximately
5
6
7 5 mg of sample were used.

8 9 **2.2.2. EGA-MS**

10
11 The instrumentation consists of a micro-furnace Multi-Shot Pyrolyzer EGA/PY-3030D (Frontier Lab Ltd.
12
13 Koriyama, JP) coupled with a 5973 Agilent Technologies mass spectrometer equipped with a deactivated
14
15 and uncoated stainless steel transfer tube (UADTM-2.5N, 0.15 mm i.d. x 2.5 m length, Frontier Lab) kept at
16
17 300 °C as well as the oven and the injector. Injector was used in split mode (20:1). A program temperature
18
19 was chosen for the micro-furnace chamber: initial temperature 50 °C; 15 °C/min up to 900 °C. The mass
20
21 spectrometer was operated in EI positive mode (70 eV, scanning m/z 50-800). The MS transfer line
22
23 temperature was 300 °C. The MS ion source temperature was kept at 230 °C and the MS quadrupole
24
25 temperature at 150 °C. For each experiment, approximately 500 µg of sample were placed into a stainless
26
27 steel cup and inserted into the micro-furnace.
28
29
30
31
32

33 34 **2.2.3. DSPy-GC/MS**

35
36
37 The instrumentation consists of a micro-furnace Multi-Shot Pyrolyzer PY-3030D (Frontier Lab Ltd. Koriyama,
38
39 JP) coupled to a gas chromatograph 6890 Agilent Technologies (Palo Alto, USA) equipped with an HP-5MS
40
41 fused silica capillary column (stationary phase 5% diphenyl-95% dimethyl-polysiloxane, 30 m x 0.25 mm i.d.,
42
43 Hewlett Packard, USA) and with a deactivated silica pre-column (2 m x 0.32 mm i.d., Agilent J&W, USA). The
44
45 GC was coupled with an Agilent 5973 Mass Selective Detector operating in electron impact mode (EI) at 70
46
47 eV. Double shot pyrolysis entails the pyrolysis of the same sample at two different temperatures. Each
48
49 sample (about 500 µg) was placed into a cup connected with the sample holder through a long stainless
50
51 steel stick and inserted into the micro-furnace. This enabled the sample to be retrieved from the pyrolysis
52
53 chamber after the first shot. DSPy temperatures were selected on the basis of maximum temperature
54
55 peaks in the EGA-MS profiles. The first shot temperature was a value between 210 – 280 °C (Thermal
56
57 Desorption duration 1 min; TD). The second shot temperature was a value between 445 – 460 °C (Pyrolysis
58
59
60
61
62
63
64
65

1 duration 1min; Py). Gases evolved at the two different temperatures were eluted in the chromatographic
2 column and detected by mass spectrometry. Chromatographic conditions of both shots were as follows:
3
4 initial temperature 50 °C, 2 min isothermal; 10 °C/min up to 300°C, 20 min isothermal. Carrier gas: He
5 (purity 99,995%), constant flow 1,1 mL/min.
6
7
8
9

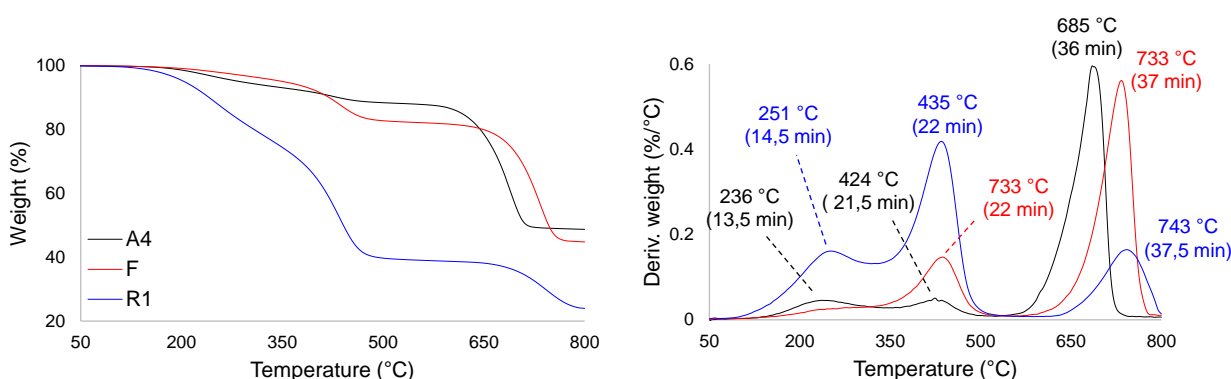
10 2.3. Multivariate statistical analysis

11
12
13 Principal component analysis (PCA) was performed via XLSTAT software using the covariance matrix. Data
14
15 matrix for the PCA was built using the relative percentages of the sum of the peak areas of principal
16
17 biomarkers detected in first and second shot of DSPy-GC/MS chromatograms. The biomarkers were
18
19 obtained from Extract Ion Chromatograms (m/z 191) characteristic of terpanes and are listed in Table 7.
20
21
22

23 3. Results and discussion

24 3.1 TG-FTIR

25
26
27 Three of the geological samples (one for each geographic area considered) were analysed by TG-FTIR to
28
29 obtain a preliminary characterization. Figure 1 shows the TG and DTG curves obtained under nitrogen for
30
31 samples A4, from Abruzzo (AQ), F, from Lazio, and R1, from Sicily. Peak DTG temperatures and mass loss
32
33 percentage of each step under nitrogen are given in Table 2.
34
35
36
37
38
39



40
41
42
43
44
45
46
47
48
49
50
51
52
53 **Figure 1** - TG (left) and DTG (right) curves obtained for sample A4, F and R1 under a stream of nitrogen of
54
55 10 °C/min.
56
57
58
59

60 **Table 2** - DTG peak temperatures and mass loss percentages for all the steps of the TG curves.
61
62
63
64
65

| | DTG peak temperature (Weight loss %) | | |
|-------------------|---|-------------------|-------------------|
| | A4 (Abruzzo) | F (Lazio) | R1 (Sicily) |
| Step 1 | 236 °C (6,5%) | - - | 251 °C (22,7%) |
| Step 2 | 424 °C (5,3%) | 437 °C (18,0%) | 435 °C (38,4%) |
| Step 3 | 685 °C (39,3%) | 733 °C (37,2%) | 743 °C (24,0%) |
| Residue at 800 °C | (48,7%) | (44,8%) | (14,8%) |

The thermal curves of samples A4 and R1 show three main degradation steps, the first in the temperature range 100-300 °C, the second between 350-500 °C, and the last at about 700°C. Sample F has only two mass losses in the same temperature ranges of second and third step of A4 and R1. The gaseous species evolved by thermal degradation of the samples were analysed with FTIR spectroscopy. Figure 2 shows the FTIR spectra of the gases evolved in the decomposition steps for sample A4, F and R1. The evolution profiles of the main gaseous compounds were monitored based on their strongest infrared bands. The profiles are shown in Figure 3 for the three samples.

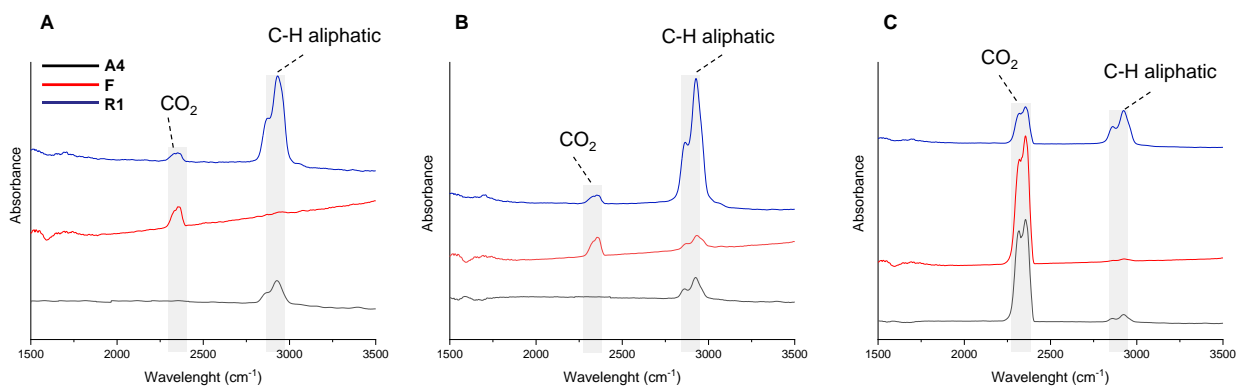


Figure 2 - FTIR spectra of the evolved gas in the range (A) 100 - 300 °C, (B) 350 - 500 °C and (C) 550 - 800 °C for sample A4, F and R1 under nitrogen flow.

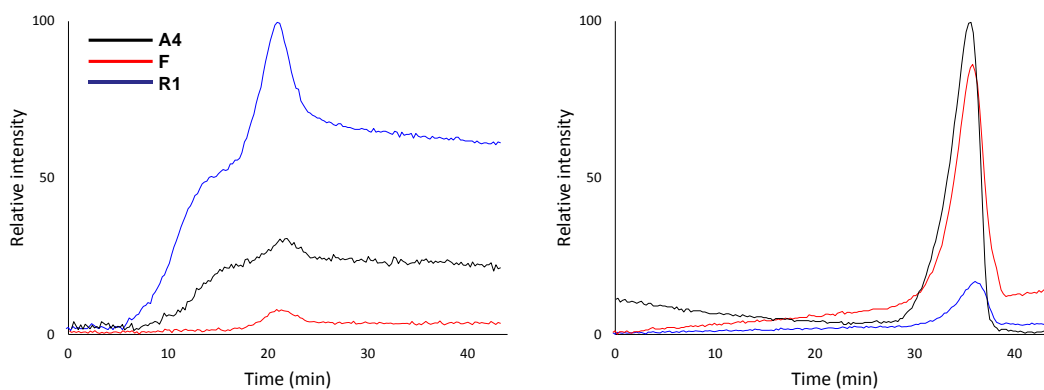


Figure 3 - Evolution profiles of (left) aliphatic compounds and (right) CO₂ in sample A4, F and R1.

The spectra show the bands of the aliphatic C-H stretching at 2968-2883 cm⁻¹ in the temperature ranges of the three degradative steps of samples A4 and R1 even though the intensity of the bands in sample R1 is much higher. Sample F presents these bands just in the second degradative step (300 – 500 °C). In addition, we identify very strong bands of CO₂ (2400-2300 cm⁻¹) at about 700°C. The presence of C-H stretching band can be related to aliphatic compounds that are evolved first at lower temperatures suggesting the presence of volatile fraction, and then at higher temperature maybe as decomposition compounds of higher molecular weight molecules. Sample F did not show evolution of aliphatic compounds at lower temperatures. This can be confirmed by examining the evolution profiles in Figure 3. The CO₂ evolved at 700 °C can be ascribed to the degradation of inorganic carbonates of the rock on which bitumen is absorbed [29]. On this respect, samples A4 and F have a residue at 900 °C higher than 45% weight indicating a high content of inorganic material, while R1 has a residue of about 15%. In order to quantify the organic fraction of the bitumen respect to the inorganic ones, we repeated the TG measurements under oxygen, and we measured the mass loss of the samples up to 600°C ascribable to the combustion of the organic material and before the degradation of the rock fragments. The organic and inorganic percent of the bitumen rocks calculated in that way are reported in Table 3 and the TG curves under oxygen are reported in Figure S1 of Supplementary Material.

Sample A4 and F have a lower quantity of organic material respect to R1, (15% vs 88%). The high quantity of organic material in R1 (up to 500°C) under nitrogen is also revealed as a cue in the spectra at 700°C not really evolved by the sample at 700°C but coming from the evolution at lower temperature.

Table 3 – Relative amount of organic and inorganic material.

| | T (°C) | % organic fraction | % inorganic fraction |
|-----------|--------|--------------------|----------------------|
| A4 | 595 | 15,9 | 84,1 |
| F | 600 | 14,2 | 85,8 |
| R1 | 560 | 88,3 | 11,7 |

3.2 EGA-MS analysis

The geological samples were subjected to evolved gas analysis (EGA-MS) in order to study their thermochemistry and select the experimental temperatures to perform DSPy-GC/MS analyses.

All samples give very similar results. The total ion thermogram (TIT) profile and the average mass spectra obtained by EGA-MS of bitumen A4, F and R1 are shown in Figure 4. Table 4 summarizes the maximum temperature of each degradation step.

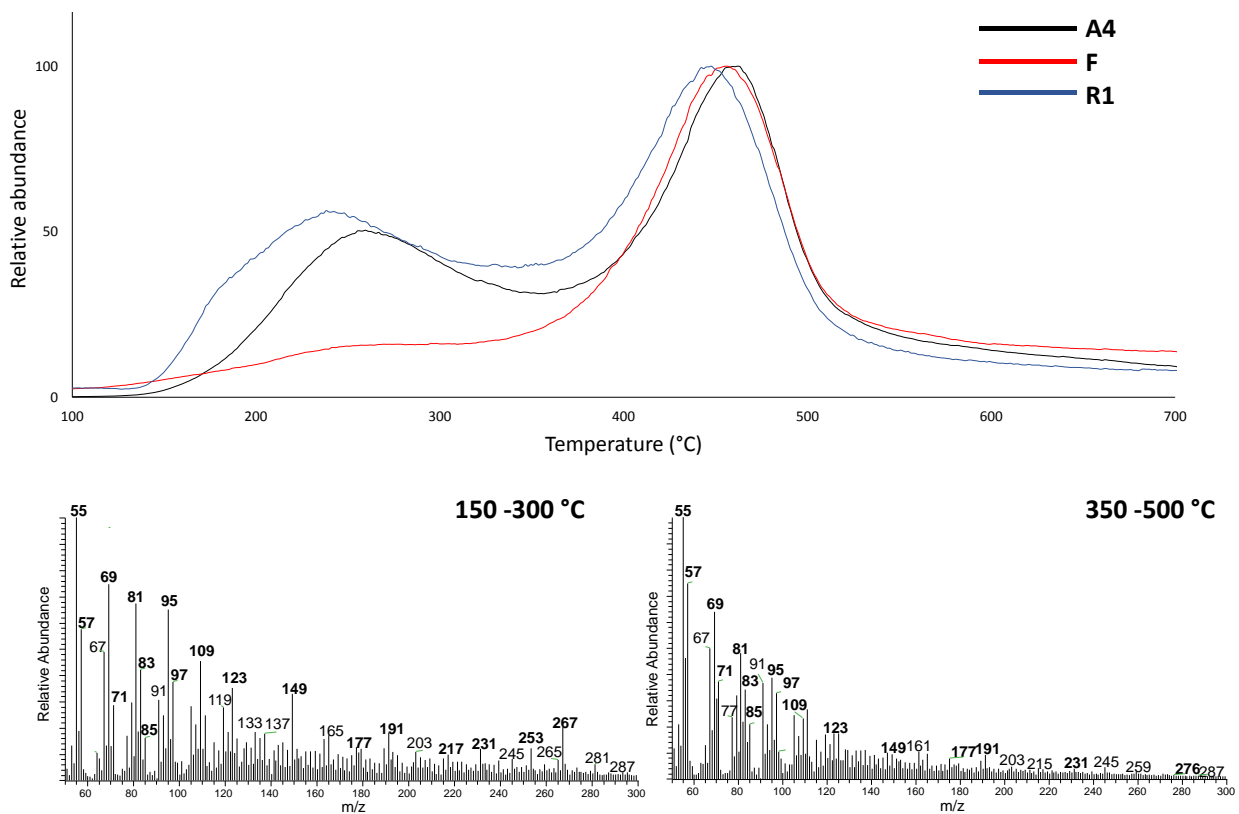


Figure 4 - Total Ion Thermogram (TIT) and average mass spectra associated of geological sample A4, F and R1.

Table 4 - Experimental temperatures of the degradation steps obtained for geological samples.

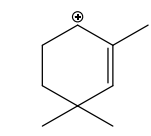
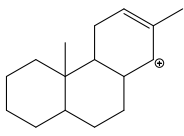
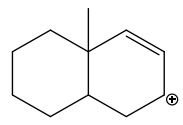
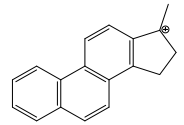
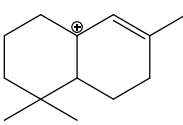
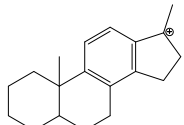
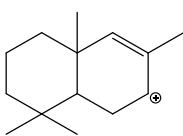
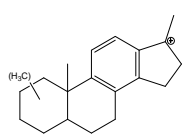
| Sample | Temperature of the maximum | |
|--------|----------------------------|---------|
| | Step #1 | Step #2 |
| A1 | 232 °C | 461 °C |
| A2 | 220 °C | 457 °C |
| A3 | 228 °C | 460 °C |
| A4 | 260 °C | 460 °C |
| A5 | 265 °C | 465 °C |
| A6 | 224 °C | 459 °C |
| R1 | 245 °C | 448 °C |
| R2 | 240 °C | 448 °C |
| R3 | 230 °C | 458 °C |
| F | 247 °C | 456 °C |

The thermograms of the geological bitumen exhibit two peaks, ascribable to two main degradation steps, in good agreement with the mass losses revealed by TG analysis. The first peak has a maximum at temperatures ranging from 220 to 265 °C and the second one from 445 to 465 °C. Given that the first step takes place at relatively low temperature, it is considered a thermal desorption process in which the smaller and more volatile compounds are released. The average mass spectrum associated to the first peak in the thermogram is dominated by the peaks due to the fragmentation of hydrocarbons as also suggested by TG-FTIR analysis. In particular, peaks at m/z 57, 71, 85 from alkanes, at m/z 55, 69, 83, 97 from alkenes and at m/z 67, 81, 95, 109 from dienes are present as well as peaks at m/z 91 and 105 from aromatic rings obtained by the rearrangements of aliphatic chains at high temperature [36]. In addition, peaks at m/z 123, 149, 177, 191, 217, 231, 253 and 267, characteristics of terpanes and steranes, can be observed. Table 5 lists the main peaks present in the mass spectra along with the structure of the corresponding ions and fragment ions and class of compounds from which they derive.

The second step takes place at higher temperature and it is considered as an actual pyrolytic process in which the polymeric network is decomposed. Nevertheless, the average mass spectrum associated to the second peak is quite similar to first one and shows peaks at the same m/z ratios. The analogies between the mass spectra corresponding to the two thermal degradation steps suggest that similar species are released during the two steps. We believe that free and more volatile compounds are desorbed during the first step (at about 250 °C), while at higher temperatures (at about 450 °C) the decomposition of the asphaltenes,

consisting in complex polycyclic structure including alkyl-substituted structures [37], is occurring. In addition, similar species could be trapped into the asphaltenic matrix and can be released when the asphaltenes decomposes.

Table 5 - List of the most abundant peaks identified in the average mass spectra of the two degradation steps along with the structure of the corresponding fragment ions and class of compounds from which they derive.

| <i>m/z</i> | Structure | Class | <i>m/z</i> | Structure | Class |
|------------|---|--------------------------|------------|--|--------------------------|
| 55 | $C_4H_7^{+\bullet}$ | Unsaturated hydrocarbons | 83 | $C_6H_{11}^{+\bullet}$ | Unsaturated hydrocarbons |
| 57 | $C_4H_9^{+\bullet}$ | Saturated hydrocarbons | 85 | $C_6H_{13}^{+\bullet}$ | Saturated hydrocarbons |
| 69 | $C_5H_9^{+\bullet}$ | Unsaturated hydrocarbons | 95 | $C_7H_{11}^{+\bullet}$ | Unsaturated hydrocarbons |
| 71 | $C_5H_{11}^{+\bullet}$ | Saturated hydrocarbons | 97 | $C_7H_{13}^{+\bullet}$ | Unsaturated hydrocarbons |
| 81 | $C_6H_9^{+\bullet}$ | Unsaturated hydrocarbons | 109 | $C_8H_{13}^{+\bullet}$ | Unsaturated hydrocarbons |
| 123 |  | Terpanes | 217 |  | Steranes |
| 149 |  | Steranes | 231 |  | Triaromatic steranes |
| 177 |  | Norhopanes | 253 |  | Monoaromatic steranes |
| 191 |  | Hopanes | 267 |  | Monoaromatic steranes |

EGA-MS analysis was performed on four archaeological samples, three from Colle Cera excavation (CC6, CC7 and CC9) and one from Catignano excavation (CT1).

Compared to geological samples thermograms, the profiles of these four samples show a single degradation step with a maximum between 445 and 460 °C (Table 6). The thermogram and the mass

spectra associated to sample CC6 are shown in Figure 5 as an example. The thermograms of the other archaeological samples are reported in Figure S2 of Supplementary Material.

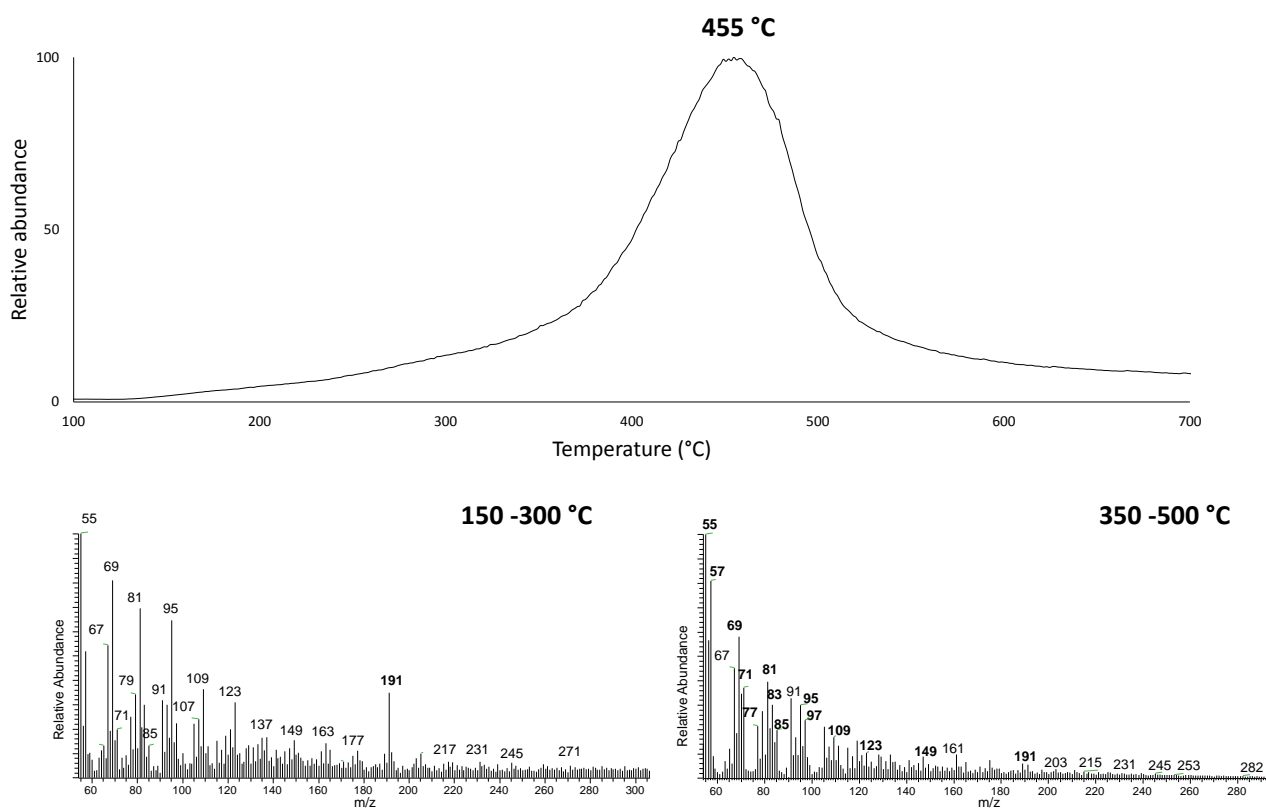


Figure 5 - Total Ion Thermogram (TIT) and average mass spectra associated of archaeological sample CC6.

The temperature range is the same than that of the second degradation step of the reference materials, suggesting the only presence of species derived from the decomposition of asphaltenic fraction. This is confirmed by the average mass spectra shown in Figure 5: the spectrum relative to the first area shows an increasing in the abundance of the peaks at m/z 191 probably due to the decreasing of the fragment ions of alkanes, alkenes, dienes and aromatic rings. On the other hand, the spectrum associated to the degradation peak has the same profile of that obtained in second step degradation of geological samples.

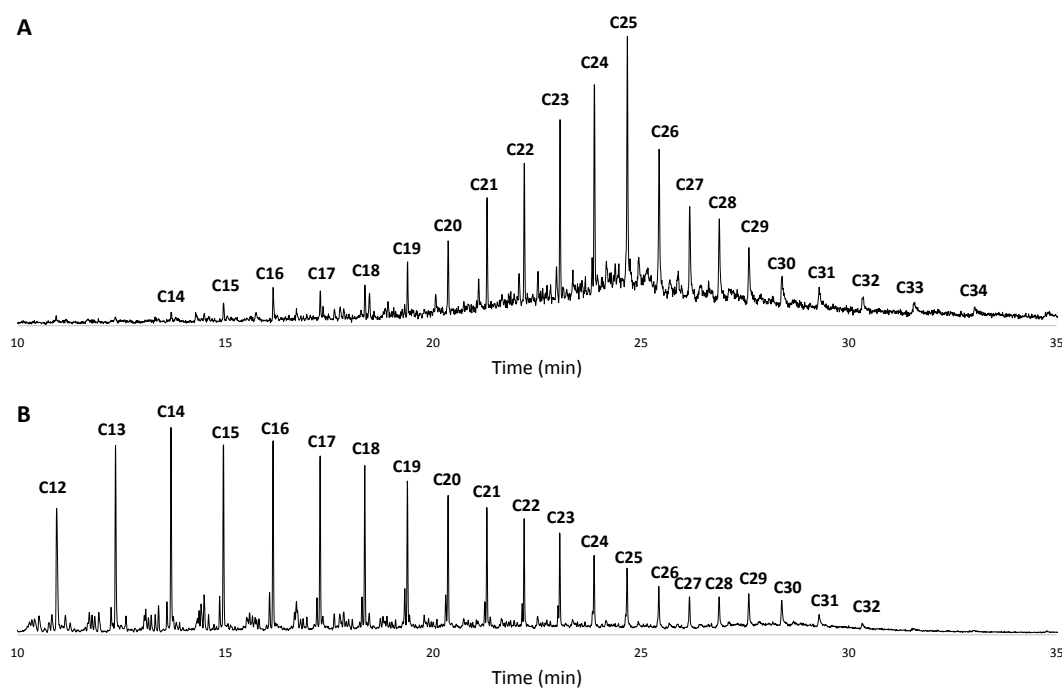
We assume that the depletion of the more volatile fraction of bitumen could have been induced by the anthropogenic treatments performed on bitumen in the interest of extracting it from the rocks and making it suitable for several applications. In particular, heating is thought to be responsible for the evaporation of more volatile compounds.

Table 6 - Experimental temperatures of the degradation steps obtained for archaeological samples.

| Sample | Temperature of the maximum |
|--------|----------------------------|
| CC6 | 455 °C |
| CC7 | 455 °C |
| CC9 | 440 °C |
| CT1 | 460 °C |

3.3 DSPy-GC/MS analysis

To further investigate the main products of thermal decomposition at the different temperatures, and thus to better understand the results obtained by TG and EGA, samples were analysed by double shot pyrolysis gas chromatography/mass spectrometry (DSPy-GC/MS). The temperatures of the two shots were selected for each sample basing on EGA-MS results: a first thermal desorption (TD) was selected in a range of 220 – 260 °C and subsequently an actual pyrolysis (Py) was performed in a range of 445 – 465 °C. As suggested by previous analysis, both the thermal desorption chromatogram and the pyrogram of the geological samples are dominated by the peaks of alkanes, alkenes and dienes. In particular, extracting the signal at m/z 85, n -alkanes ranging from 11 to 34 carbon atoms can be identified. Figure 6 reports the result obtained for geological sample A4 as an example, same results were obtained for other samples investigated.



1
2
3
4
5
6
7
8
9
10
11
12
13
14
15
16
17
18
19
20
21
22
23
24
25
26
27
28
29
30
31
32
33
34
35
36
37
38
39
40
41
42
43
44
45
46
47
48
49
50
51
52
53
54
55
56
57
58
59
60
61
62
63
64
65

Figure 6 - DSPy-GC/MS extract ion chromatograms (m/z 85) at (A) 260 °C and (B) 460 °C of geological sample A4. Cn: linear alkane with n carbon atoms.

For archaeological samples, analyses were performed in double shot mode, despite the lack of the first degradation step, showing that alkanes are absent in the chromatogram of thermal desorption temperature range (Figure 7) supporting the results obtained from EGA-MS analysis.

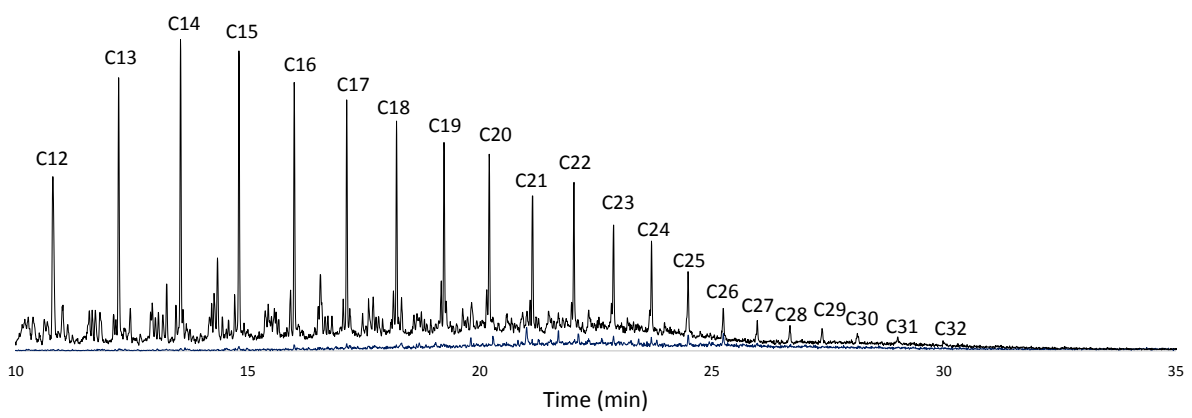


Figure 7 - Double shot Py-GC/MS extract ion chromatograms (m/z 85) of the archaeological sample CC6 at 250 °C (blue line) and at 460 °C (black line). Cn: linear alkane with n carbon atoms.

Given that analytical pyrolysis requires small amount of sample which does not need any pre-treatments we decided to test this technique to establish if it is suitable for biomarker analysis. To this purpose, terpane distribution pattern (m/z 191) was used. Chromatographic profiles obtained for the geological and archaeological samples at the temperatures of 250 °C and 460 °C are shown in Figure 8 and Figure 9, respectively. Table 7 lists the identified biomarkers.

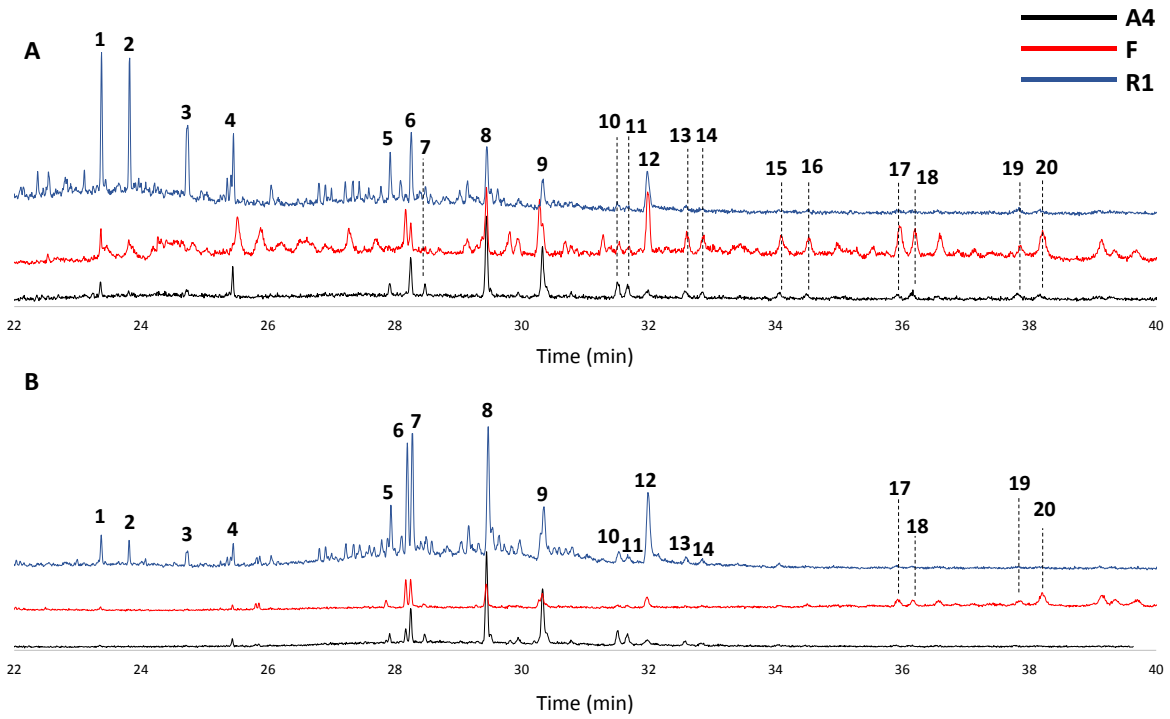


Figure 8 - Double shot Py-GC/MS extract ion chromatograms (m/z 191) at (A) 250 °C and (B) 460 °C of geological sample A4, F and R1. Peaks are labelled according to Table 7.

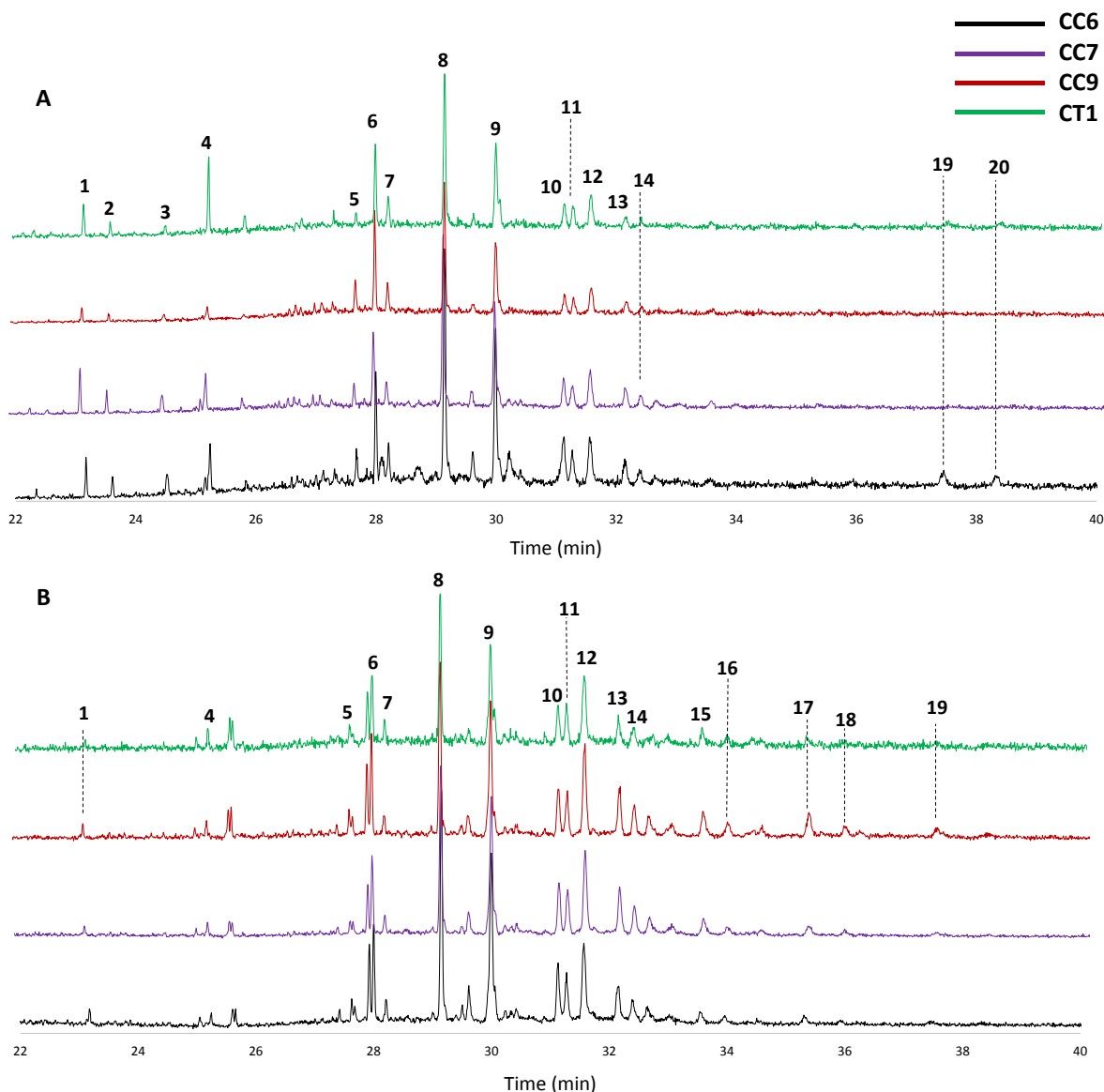


Figure 9 - Double shot Py-GC/MS extract ion chromatograms (m/z 191) at (A) 250 °C and (B) 460 °C of archaeological sample CC6, CC7, CC9 and CT1. Peaks are labelled according to Table 7.

Table 7 - Principal compounds detected in thermal desorption chromatograms and pyrograms of geological and archaeological samples.

| Peak number | Compound | Abbreviation |
|-------------|---|--------------|
| 1 | C23 tricyclic terpene | TR23 |
| 2 | C24 tricyclic terpene | TR24 |
| 3 | C25 tricyclic terpene | TR25 |
| 4 | C24 tetracyclic terpene | TET24 |
| 5 | 18 α (H),21 β (H)-22,29,30-trisnorhopane | Ts |
| 6 | 17 α (H),18 α (H),21 β (H)-22,29,30-trisnorhopane | Tm |
| 7 | 17 α (H),18 α (H),21 β (H)-28,30-bisnorhopane | H28 |

| | | |
|----|--|------|
| 8 | 17 α (H),21 β (H)-30-norhopane | H29 |
| 9 | 17 α (H),21 β (H)-hopane | H30 |
| 10 | 22S-17 α (H),21 β (H)-30-homohopane | H31S |
| 11 | 22R-17 α (H),21 β (H)-30-homohopane | H31R |
| 12 | Gammacerane | GAM |
| 13 | 22S-17 α (H),21 β (H)-30,31-bishomohopane | H32S |
| 14 | 22R-17 α (H),21 β (H)-30,31-bishomohopane | H32R |
| 15 | 22S-17 α (H),21 β (H)-30,31,32-trishomohopane | H33S |
| 16 | 22R-17 α (H),21 β (H)-30,31,32-trishomohopane | H33R |
| 17 | 22S-17 α (H),21 β (H)-30,31,32,33-tetrakishomohopane | H34S |
| 18 | 22R-17 α (H),21 β (H)-30,31,32,33-tetrakishomohopane | H34R |
| 19 | 22S-17 α (H),21 β (H)-30,31,32,33,34-pentakishomohopane | H35S |
| 20 | 22R-17 α (H),21 β (H)-30,31,32,33,34-pentakishomohopane | H35R |

Several biomarkers were identified in the chromatographic profiles despite the low resolution and the small abundance of the peaks. Table S1 of Supplementary Material reports the relative abundance of the biomarker identified in the first and second shot of DSPy-GC/MS of the investigated samples.

To highlight the compositional differences, data obtained were submitted to multivariate statistical analysis by principal component analysis (PCA). The resulting scatter and loading plots for the first two principal components are shown in Figure 10.

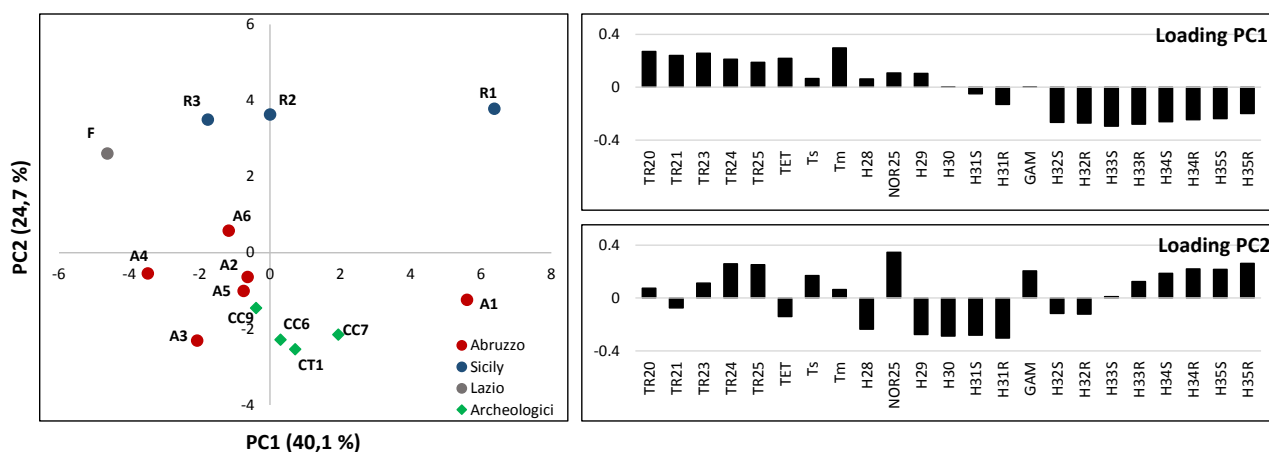


Figure 10 - PCA scatter plot and loading plot of the chromatographic data obtained by DSPy-GC/MS for the geological and archaeological samples analysed.

PC1 and PC2 account for 64,8% of the variance. The samples in the plot get separated on PC2: samples from Sicily and Lazio are located at positive values of PC2, while archaeological and geological samples from Abruzzo are located at values of PC2 lower than 1. The abundance of gammacerane (GAM) and

1 trisorhopanes (Ts and Tm) characterises the samples from Sicily and Lazio, while samples from Abruzzo are
2 enriched in hopane and homohopane homologs (H28 – H31) and are characterized by the lack of 25-
3
4 norhopane (NOR25H). Although the separation is not so pronounced, pyrolysis data allow us to
5
6 discriminate the different bitumen source and to state that archaeological samples share the origin with
7
8 bitumen from Abruzzo. These results are consistent with those achieved by GC/MS [20], thus proving the
9
10 suitability of the proposed method based on analytical pyrolysis to study bitumen and its origin
11
12 identification.
13
14
15

16 **4. Conclusions**

17
18 Data and results obtained within this work show how the use of the combination of thermal analysis and
19
20 analytical pyrolysis, used into two different configurations, EGA-MS and DSPy-GC/MS, is an extremely
21
22 effective way to chemically characterize bituminous samples. Above all, it has been proven the suitability of
23
24 such approach for the study of bitumen, in particular of archaeological bitumen, since the techniques used
25
26 requires significantly low amounts of sample and no sample pre-treatment.
27
28
29
30

31 The thermochemistry and the thermal-complexity of bitumen samples were investigated by TG-FTIR and
32
33 EGA-MS, allowing us to highlight the main degradative patterns and the main differences among samples
34
35 coming from different geographical zones and to emphasize the differences between geological and
36
37 archaeological samples. The data show that geological bitumen decomposes with two main degradation
38
39 steps peaked in the temperature range 100-300 °C and 350-500 °C, respectively during which the same kind
40
41 of compounds is evolved. These compounds are present in the samples as free species, which are desorbed
42
43 at lower temperature, and either can derive from asphaltenes decomposition at higher temperatures.
44
45
46
47

48 Archaeological samples show a single degradation step peaked at 445-465 °C. The lack of the more volatile
49
50 fraction of bitumen is probably due to the evaporation caused by the anthropogenic treatments performed
51
52 on bitumen in the interest of extracting it from the rocks and making it suitable for its several applications.
53

54 Double shot pyrolysis gas chromatography/mass spectrometry (DSPy-GC/MS) was used to deepen the TGA-
55
56 FTIR and EGA-MS data and to outline the chemical composition of the samples. The lack of the more
57
58 volatile fraction in the archaeological bitumen was confirmed analysing alkanes distribution pattern (m/z
59
60
61
62
63
64
65

85). In addition, examining the distribution profile (m/z 191) of the terpane compounds, we were able to identify more than 20 biomarkers, whose chromatographic areas were used as variables for PCA allowing us to discriminate among bitumen from different Italian geological area and to assess the origin of the archaeological bitumen.

Acknowledgements

The authors would like to thank Prof. Carlo Tozzi (University of Pisa) for giving them the opportunity to study the archaeological samples investigated in this paper. Silvia Pizzimenti (University of Pisa) is acknowledged for the help in performing thermal analysis and data treatment.

References

- [1] R.C. Selley, *Elements of petroleum geology*, Gulf Professional Publishing, 1998.
- [2] M. Cârciumar, R.-M. Ion, E.-C. Nițu, R. Ștefănescu, New evidence of adhesive as hafting material on Middle and Upper Palaeolithic artefacts from Gura Cheii-Râșnov Cave (Romania), *J. Archaeol. Sci.* 39 (2012) 1942–1950.
- [3] M. Faraco, A. Pennetta, D. Fico, G. Eramo, E. Beqiraj, I.M. Muntoni, G.E. De Benedetto, Bitumen in potsherds from two Apulian Bronze Age settlements, Monopoli and Torre Santa Sabina: composition and origin, *Org. Geochem.* 93 (2016) 22–31.
- [4] M. Olivares, M. Irazola, X. Murelaga, J.I. Baceta, A. Tarriño, K. Castro, N. Etxebarria, Sourcing sedimentary cherts with archaeological use through the combination of chromatographic and spectroscopic techniques, *Appl. Geochemistry.* 33 (2013) 252–259.
- [5] E. Boëda, S. Bonilauri, J. Connan, D. Jarvie, N. Mercier, M. Tobey, H. Valladas, H. Al Sakhel, S. Muhesen, Middle Palaeolithic bitumen use at Umm el Tlel around 70 000 BP, *Antiquity.* 82 (2008) 853–861.
- [6] J. Connan, T. Van de Velde, An overview of bitumen trade in the Near East from the Neolithic (c. 8000 BC) to the early Islamic period, *Arab. Archaeol. Epigr.* 21 (2010) 1–19.
- [7] J. Connan, O. Deschesne, *Le bitume à Suse: collection du Musée du Louvre= Bitumen at Susa, Réunion des musées nationaux*, 1996.
- [8] A. Hauser, H. Dashti, Z.H. Khan, Identification of biomarker compounds in selected Kuwait crude oils, *Fuel.* 78 (1999) 1483–1488.
- [9] J.M. Hunt, R.P. Philp, K.A. Kvenvolden, Early developments in petroleum geochemistry, *Org. Geochem.* 33 (2002) 1025–1052.
- [10] K.E. Peters, K.E. Peters, C.C. Walters, J.M. Moldowan, *The biomarker guide*, Cambridge University Press, 2005.
- [11] M. Do Lewan, Factors controlling the proportionality of vanadium to nickel in crude oils, *Geochim. Cosmochim. Acta.* 48 (1984) 2231–2238.
- [12] J. Connan, O. Deschesne, *Le bitume dans l'antiquité*, Rech. (Paris, 1970). (1991) 152–159.
- [13] A. Pennetta, D. Fico, G. Eramo, I.M. Muntoni, G.E. De Benedetto, Extending the inter-Adriatic trade of bitumen beyond the fifth millennium BCE, *Org. Geochem.* (2020) 104013.
- [14] A. Charrié-Duhaut, P. Burger, J. Maurer, J. Connan, P. Albrecht, Molecular and isotopic archaeology: top grade tools to investigate organic archaeological materials, *Comptes Rendus Chim.* 12 (2009) 1140–1153.
- [15] J. Connan, G. Kozbe, O. Kavak, J. Zumberge, K. Imbus, The bituminous mixtures of Kavușan Höyük (SE Turkey) from the end of the 3rd millennium (2000 BC) to the Medieval period (AD 14th century): Composition and origin, *Org. Geochem.* 54 (2013) 2–18.

- 1 [16] J. Łucejko, J. Connan, S. Orsini, E. Ribechini, F. Modugno, Chemical analyses of Egyptian
2 mummification balms and organic residues from storage jars dated from the Old Kingdom to the
3 Copto-Byzantine period, *J. Archaeol. Sci.* 85 (2017) 1–12. <https://doi.org/10.1016/j.jas.2017.06.015>.
- 4 [17] K. Grice, S. Schouten, K.E. Peters, J.S.S. Damsté, Molecular isotopic characterisation of hydrocarbon
5 biomarkers in Palaeocene–Eocene evaporitic, lacustrine source rocks from the Jiangnan Basin,
6 China, *Org. Geochem.* 29 (1998) 1745–1764.
- 7 [18] P. Avramidis, A. Zelilidis, Potential source rocks, organic geochemistry and thermal maturation in the
8 southern depocenter (Kipourio–Grevena) of the Mesohellenic Basin, central Greece, *Int. J. Coal
9 Geol.* 71 (2007) 554–567.
- 10 [19] J. Connan, O. Kavak, E. Akin, M.N. Yalçin, K. Imbus, J. Zumberge, Identification and origin of bitumen
11 in Neolithic artefacts from Demirköy Höyük (8100 BC): Comparison with oil seeps and crude oils
12 from southeastern Turkey, *Org. Geochem.* 37 (2006) 1752–1767.
- 13 [20] F. Nardella, N. Landi, I. Degano, M. Colombo, M. Serradimigni, C. Tozzi, E. Ribechini, Chemical
14 investigations of bitumen from Neolithic archaeological excavations in Italy by GC/MS combined
15 with principal component analysis, *Anal. Methods.* 11 (2019). <https://doi.org/10.1039/c8ay02429d>.
- 16 [21] I. Degano, F. Modugno, I. Bonaduce, E. Ribechini, M.P. Colombini, Recent advances in analytical
17 pyrolysis to investigate organic materials in heritage science, *Angew. Chemie Int. Ed.* 57 (2018)
18 7313–7323.
- 19 [22] S. Orsini, F. Parlanti, I. Bonaduce, Analytical pyrolysis of proteins in samples from artistic and
20 archaeological objects, *J. Anal. Appl. Pyrolysis.* 124 (2017) 643–657.
21 <https://doi.org/10.1016/j.jaap.2016.12.017>.
- 22 [23] E. Ribechini, M. Bacchiocchi, T. Deviese, M.P. Colombini, Analytical pyrolysis with in situ thermally
23 assisted derivatisation, Py (HMDS)-GC/MS, for the chemical characterization of archaeological birch
24 bark tar, *J. Anal. Appl. Pyrolysis.* 91 (2011) 219–223.
- 25 [24] M.P. Colombini, E. Ribechini, M. Rocchi, P. Selleri, Analytical pyrolysis with in-situ silylation, Py
26 (HMDS)-GC/MS, for the chemical characterization of archaeological and historical amber objects,
27 *Herit. Sci.* 1 (2013) 6.
- 28 [25] M. Mattonai, A. Watanabe, E. Ribechini, Characterization of volatile and non-volatile fractions of
29 spices using evolved gas analysis and multi-shot analytical pyrolysis, *Microchem. J.* 159 (2020)
30 105321.
- 31 [26] M.R. Tiné, C. Duce, Calorimetric and Thermoanalytical Techniques in the Study of Ageing
32 Phenomena and Molecular Interaction in Paintings, in: *Nanotechnologies Nanomater. Diagnostic,
33 Conserv. Restor. Cult. Herit.*, Elsevier, 2019: pp. 79–109.
- 34 [27] A. Lluveras-Tenorio, A. Spepi, M. Pieraccioni, S. Legnaioli, G. Lorenzetti, V. Palleschi, M. Vendrell,
35 M.P. Colombini, M.R. Tiné, C. Duce, A multi-analytical characterization of artists' carbon-based black
36 pigments, *J. Therm. Anal. Calorim.* 138 (2019) 3287–3299.
- 37 [28] S. Orsini, C. Duce, I. Bonaduce, Analytical pyrolysis of ovalbumin, *J. Anal. Appl. Pyrolysis.* 130 (2018)
38 62–71.
- 39 [29] C. Duce, S. Orsini, A. Spepi, M.P. Colombini, M.R. Tiné, E. Ribechini, Thermal degradation chemistry
40 of archaeological pine pitch containing beeswax as an additive, *J. Anal. Appl. Pyrolysis.* 111 (2015)
41 254–264. <https://doi.org/10.1016/j.jaap.2014.10.020>.
- 42 [30] M. Fiedlerová, P. Jíša, D. Kadlec, R. Velvarská, K. Štěpánek, Using various thermal analytical methods
43 for bitumen characterization, *Int. J. Pavement Res. Technol.* 14 (2021) 459–465.
- 44 [31] G.M. Languri, J. van der Horst, J.J. Boon, Characterisation of a unique 'asphalt' sample from the early
45 19th century Hafkenscheid painting materials collection by analytical pyrolysis MS and GC/MS, *J.
46 Anal. Appl. Pyrolysis.* 63 (2002) 171–196.
- 47 [32] F.F. Cazzini, The history of the upstream oil and gas industry in Italy, *Geol. Soc. London, Spec. Publ.*
48 465 (2018) 243–274.
- 49 [33] F. Gerali, L. Lipparini, Maiella, an oil massif in the Central Apennines ridge of Italy: exploration,
50 production and innovation in the oil fields of Abruzzo across the nineteenth and twentieth
51 centuries, *Geol. Soc. London, Spec. Publ.* 465 (2018) 275–303.
- 52 [34] M. Colombo, M. Serradimigni, C. Tozzi, Un nuovo villaggio della cultura di Catignano: il sito di Colle
53 Cera presso Loreto Aprutino (Pescara), *Orig. Preist. e Protostoria Delle Civiltà Antiche.* (2008) 57–98.
- 54
55
56
57
58
59
60
61
62
63
64
65

- 1 [35] C. TOZZI, B. ZAMAGNI, Gli scavi nel villaggio neolitico di Catignano (1971-1980), (2003).
2 [36] D. Tamburini, J.J. Łucejko, F. Modugno, M.P. Colombini, Combined pyrolysis-based techniques to
3 evaluate the state of preservation of archaeological wood in the presence of consolidating agents, J.
4 Anal. Appl. Pyrolysis. 122 (2016) 429–441. <https://doi.org/10.1016/j.jaap.2016.10.026>.
5 [37] P.G. Redelius, The structure of asphaltenes in bitumen, Road Mater. Pavement Des. 7 (2006) 143–
6 162.
7
8
9
10
11
12
13
14
15
16
17
18
19
20
21
22
23
24
25
26
27
28
29
30
31
32
33
34
35
36
37
38
39
40
41
42
43
44
45
46

47 **Supplementary Material**

48 **Analytical pyrolysis and thermal analysis to chemically characterise bitumen from** 49 50 51 52 53 **Italian geological deposits and Neolithic stone tools**

54
55
56
57 **Figure S1** - TG (left) and DTG (right) curves obtained for sample A4 (Abruzzo, AQ), F (Lazio) and R1 (Sicily)
58 under a stream of air of 20 °C/min.
59
60
61
62
63
64
65

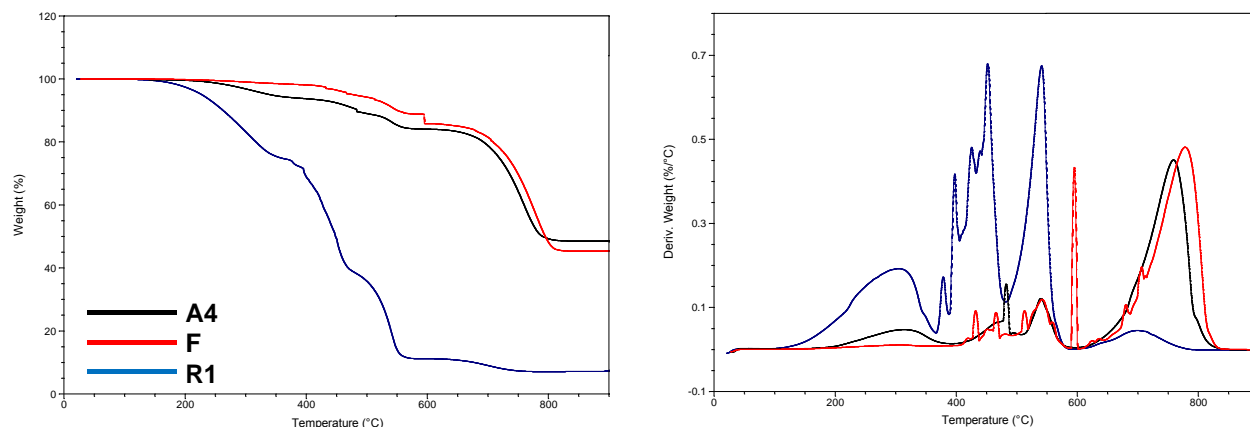


Figure S2 - Thermograms of archaeological samples (A) CC7, (B) CC9 and (C) CT1.

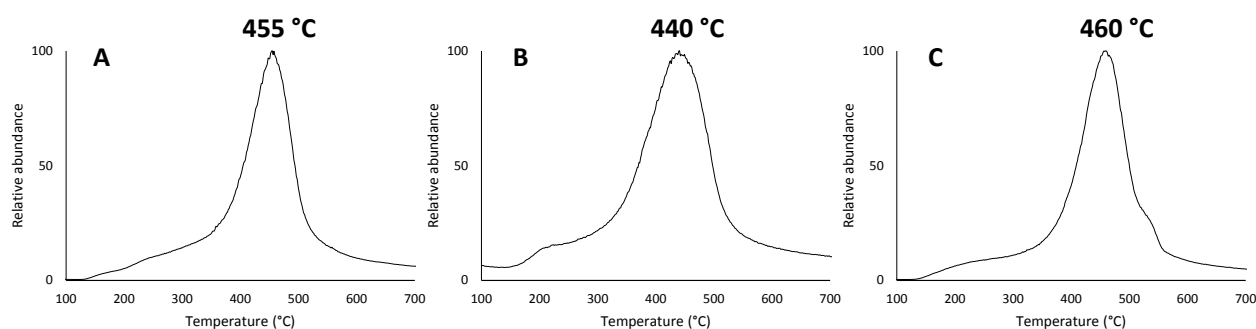


Table S1 - Relative abundance of biomarker identified in first and second shot of DSPy-GC/MS of the samples investigated.

| | A1 | A2 | A3 | A4 | A5 | A6 | R1 | R2 | R3 | F | CT1 | CC7 | CC6 | CC9 |
|-------|------|------|------|------|------|------|------|------|------|-----|------|------|------|------|
| TR20 | 6.2 | 0.0 | 0.0 | 0.0 | 0.0 | 0.0 | 5.0 | 0.0 | 0.0 | 0.0 | 0.0 | 0.0 | 0.0 | 0.0 |
| TR21 | 1.7 | 0.0 | 0.0 | 0.0 | 0.0 | 0.7 | 3.6 | 0.0 | 0.0 | 0.0 | 2.5 | 1.8 | 2.3 | 2.5 |
| TR23 | 6.9 | 4.5 | 0.3 | 1.3 | 1.9 | 3.1 | 5.3 | 3.9 | 2.6 | 0.5 | 2.3 | 2.4 | 1.4 | 1.2 |
| TR24 | 1.0 | 0.0 | 0.0 | 0.0 | 0.0 | 0.6 | 4.8 | 1.8 | 2.6 | 0.0 | 0.9 | 1.5 | 0.5 | 0.3 |
| TR25 | 0.0 | 0.0 | 0.0 | 0.0 | 0.0 | 0.0 | 4.7 | 1.7 | 1.7 | 0.0 | 0.0 | 1.5 | 0.7 | 0.4 |
| TET | 8.3 | 3.7 | 0.4 | 2.9 | 1.2 | 2.2 | 3.1 | 2.0 | 1.2 | 0.6 | 6.0 | 4.1 | 2.3 | 2.1 |
| Ts | 2.5 | 1.7 | 0.9 | 1.9 | 4.7 | 1.0 | 3.8 | 4.0 | 4.0 | 3.6 | 1.9 | 5.1 | 1.7 | 2.8 |
| Tm | 18.0 | 14.2 | 7.1 | 8.7 | 13.5 | 12.5 | 20.5 | 13.1 | 10.5 | 8.8 | 11.8 | 16.3 | 10.9 | 13.2 |
| H28 | 5.3 | 4.0 | 2.3 | 2.2 | 3.4 | 3.1 | 0.0 | 0.0 | 0.0 | 2.5 | 3.6 | 13.4 | 2.6 | 2.5 |
| NOR25 | 0.0 | 0.0 | 0.0 | 0.0 | 0.0 | 0.0 | 3.2 | 2.9 | 2.5 | 0.0 | 0.0 | 0.0 | 0.0 | 0.0 |
| H29 | 24.9 | 20.4 | 21.1 | 15.7 | 24.7 | 18.8 | 15.2 | 13.3 | 8.2 | 9.2 | 20.1 | 12.6 | 20.9 | 17.4 |
| H30 | 15.6 | 10.1 | 21.7 | 11.8 | 15.3 | 8.3 | 9.8 | 7.9 | 10.2 | 9.9 | 14.9 | 9.7 | 19.8 | 16.1 |
| H31S | 2.8 | 4.8 | 7.0 | 5.7 | 4.4 | 3.9 | 2.2 | 4.3 | 4.1 | 2.9 | 6.1 | 10.2 | 7.1 | 5.7 |
| H31R | 2.2 | 5.0 | 6.5 | 6.0 | 4.1 | 4.4 | 1.5 | 3.5 | 3.6 | 2.1 | 5.8 | 6.0 | 5.1 | 4.9 |
| GAM | 2.6 | 4.7 | 9.0 | 4.2 | 2.7 | 9.8 | 13.0 | 11.2 | 10.9 | 9.5 | 10.3 | 5.6 | 9.5 | 10.5 |
| H32S | 1.0 | 2.9 | 4.1 | 4.5 | 3.0 | 3.3 | 1.5 | 2.6 | 3.8 | 4.6 | 4.3 | 3.5 | 3.9 | 4.7 |
| H32R | 0.9 | 2.4 | 3.2 | 4.1 | 3.7 | 2.9 | 1.0 | 1.7 | 3.3 | 4.1 | 4.0 | 2.3 | 3.3 | 3.6 |
| H33S | 0.0 | 5.5 | 3.5 | 6.3 | 3.7 | 3.4 | 0.0 | 2.2 | 4.5 | 5.4 | 2.3 | 2.2 | 1.8 | 3.5 |
| H33R | 0.0 | 3.8 | 2.2 | 5.3 | 3.1 | 2.3 | 0.0 | 3.0 | 3.9 | 7.8 | 1.7 | 1.8 | 1.1 | 2.1 |
| H34S | 0.0 | 4.6 | 2.9 | 3.5 | 2.1 | 3.8 | 0.0 | 5.0 | 4.4 | 8.8 | 1.6 | 0.0 | 1.4 | 3.2 |
| H34R | 0.0 | 4.0 | 2.4 | 3.9 | 4.3 | 6.1 | 0.0 | 4.4 | 6.3 | 7.2 | 0.0 | 0.0 | 0.8 | 1.3 |
| H35S | 0.0 | 4.0 | 2.6 | 7.3 | 2.7 | 6.6 | 0.8 | 4.8 | 7.9 | 5.9 | 0.0 | 0.0 | 2.2 | 1.9 |

| H35R | 0.0 | 0.0 | 2.8 | 4.5 | 1.6 | 3.0 | 0.8 | 6.7 | 3.6 | 6.6 | 0.0 | 0.0 | 0.7 | 0.0 |
|-------------|-----|-----|-----|-----|-----|-----|-----|-----|-----|-----|-----|-----|-----|-----|
|-------------|-----|-----|-----|-----|-----|-----|-----|-----|-----|-----|-----|-----|-----|-----|

1
2
3
4
5
6
7
8
9
10
11
12
13
14
15
16
17
18
19
20
21
22
23
24
25
26
27
28
29
30
31
32
33
34
35
36
37
38
39
40
41
42
43
44
45
46
47
48
49
50
51
52
53
54
55
56
57
58
59
60
61
62
63
64
65